

## Experimental Investigation on Cross Flow of Wedge-shaped Gap in the core of Prismatic VHTR

Jeong-Hun Lee<sup>a</sup>, Su-Jong Yoon<sup>b</sup>, Goon-Cherl Park<sup>a</sup>, Hyoung-Kyu Cho<sup>a\*</sup>

<sup>a</sup>Department of Nuclear Engineering, Seoul National University, 1 Gwanak-ro, Gwanak-gu, Seoul 151-744

<sup>b</sup>Idaho National Laboratory, 2525 Fremont Avenue, Idaho Falls, USA

\*Corresponding author: *chohk@snu.ac.kr*

### 1. Introduction

Very High Temperature Reactor (VHTR), one of the Generation-IV (Gen-IV) reactors, is uranium-fueled, graphite-moderated and helium-cooled reactor. It has several advantages over the previous generation reactor; these include enhanced fuel integrity, proliferation resistance, relatively simple fuel cycle and modularity to supply electricity [1]. Prismatic modular reactor (PMR) is one of the prospective VHTR core type candidates. PMR200 is considered as a candidate for the Nuclear Hydrogen Development and Demonstration plant [2]. The core of the PMR type reactor consists of assemblies of hexagonal graphite blocks. The graphite blocks have lots of advantages for neutron economy and high temperature structural integrity [3]. The height and flat-to-flat width of fuel block are 793 mm and 360 mm, respectively. Each block has 108 coolant channels of which the diameter is 16 mm. And there are gaps between blocks not only vertically but also horizontally for reloading of the fuel elements. The vertical gap induces the bypass flow and through the horizontal gap the cross flow is formed. Since the complicated flow distribution occurs by the bypass flow and cross flow, flow characteristics in the core of the PMR reactor cannot be treated as a simple pipe flow.

The fuel zone of the PMR core consists of multiple layers of fuel blocks. The shape change of the fuel blocks could be caused by the thermal expansion and fast-neutron induced shrinkage. It could make different axial shrinkage of fuel block and this leads to wedge-shaped gaps between two stacked fuel blocks. The cross flow is often considered as a leakage flow through the horizontal gap between stacked fuel blocks and it complicates the flow distribution in the reactor core by connecting the coolant channel and the bypass gap. Moreover, the cross flow could lead to uneven coolant distribution and consequently cause superheating of individual fuel element zones with increased fission product release. Since the core cross flow has a negative impact on safety and efficiency of VHTR, core cross flow phenomena have to be investigated to improve the core thermal margin of VHTR [4]. For this reason, studies on cross flow were conducted by Groehn (1982) in Germany [5] and Kaburaki (1990) in Japan [6]. However, the shape of fuel blocks in previous study differs from that of NHDD PMR200 fuel block and the cross flow loss coefficient for PMR200 core has not been studied sufficiently. To develop the cross flow loss coefficient model for

determination of the flow distribution for PMR core analysis codes, study on cross flow for PMR200 core is essential. In particular, to predict the amount of flow through the cross flow gap, obtaining accurate flow loss coefficient is important.

In this study, the full-scale cross flow experimental facility was constructed to represent the cross flow phenomena of two stacked fuel blocks and the modifiable gap is introduced between fuel blocks. Cross flow was evaluated from the difference between measured outlet flow and inlet flow. Using the experimental results, ANSYS CFX 13 which is commercial computational fluid dynamics code was validated to confirm the applicability of the CFD analysis on the cross flow phenomena. Furthermore, characteristics of cross flow is discussed in this paper.

### 2. Cross Flow Experiment for Core of PMR200

In order to understand cross flow phenomena, cross flow experiment was designed and the full-scale two stacked fuel blocks experimental facility was constructed. Wedge-shaped gap was formed between two fuel elements. The schematic view of experimental apparatus was illustrated in Fig. 1. Air at ambient conditions was used as working fluid. The air flows through the test section from upstream block to downstream block and discharged through the blower which is connected to the bottom of the test section. Inlet flow rate of upstream block, outlet flow rate of downstream block, static pressures in coolant channels and pressure distribution in cross gap can be measured in this experimental facility. Cross flow rate can be evaluated from the difference between measured outlet flow rate and inlet flow rate. Averaging Pitot Tubes using 5 pressure ports on the upstream part and single static pressure port for the downstream part were installed for measuring inlet flow rate and outlet flow rate. Pressure transmitters were used to measure static pressures in coolant channels and in the cross gap. The measuring instruments were listed in Table 1. Test section was designed to be able to change the shape of the cross gap as depicted in Fig. 2. Wedge-shaped gap was simulated and the sizes of the gaps were selected to be 0.5, 1, 2, 4 and 6 mm. Outlet flow rates were set to be 0.1 ~ 1.35 kg/s which are evaluated to be ranged between 4000 and 54000 in Reynolds numbers at coolant channel. Since Reynolds number under normal operation condition at coolant channel of PMR200 is

approximately 23000, the test conditions can cover the normal operation condition sufficiently.

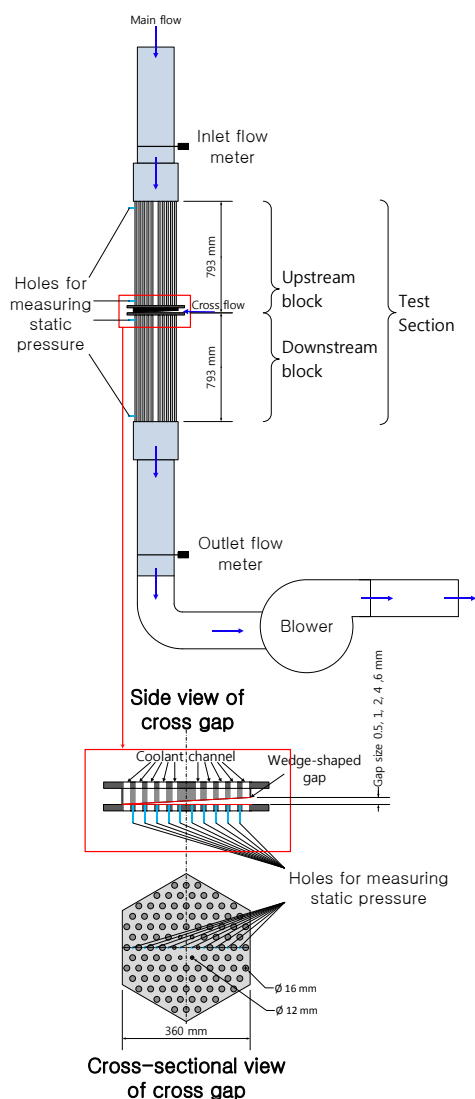


Fig. 1. Schematic view of experimental apparatus

Table 1: Measuring instruments

Variable	Measuring instrument	Error
Flow rate	FCO68 / Furness Control	0.1%
Pressure Transmitter for flow rate	Rosemount 3051 / Rosemount	0.04%
Static Pressure	VPRN-A2-(5- -10)KPa-4C / Valcom	0.1%

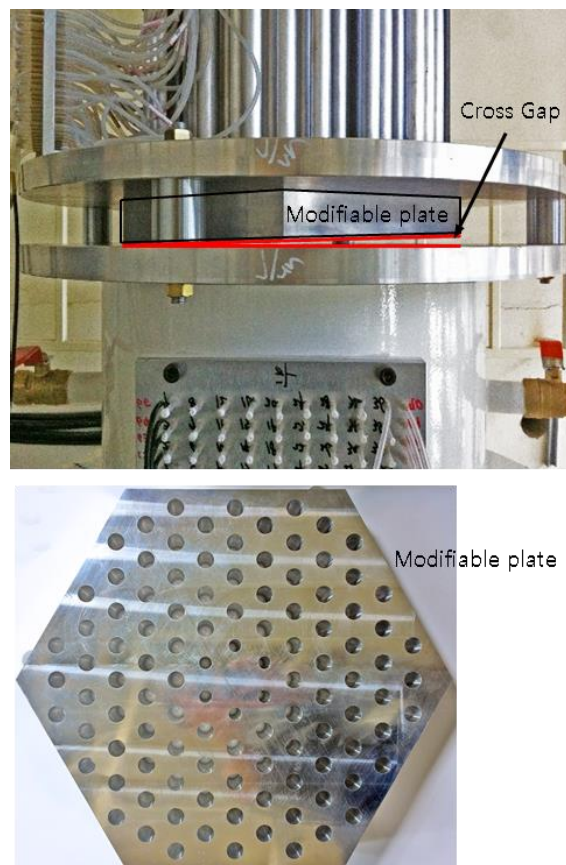


Fig. 2. Experimental apparatus and cross gap

### 3. CFD Analysis

Computational Fluid Dynamics (CFD) analysis could be used as great tools for understanding the cross flow phenomena. To apply the CFD code on the cross flow phenomena, the prediction capability of CFX 13, a commercial CFD code, was verified by comparing the predictions with the experimental data. Fig. 3 shows computational domain and mesh structure for the case of wedge-shaped gap with 0.6 mm gap size. In the present simulation, GAMBIT 2.2.30 was used for generating geometry and mesh grid. Approximately 9 million nodes of hexahedra mesh were used for the present simulation. Since the simulation with 4.2 million cell grids showed good results in our previous study [7], the finer grid system was believed to guarantee reliable calculation results. In order to enhance accuracy of the analysis results, higher mesh density was applied to the cross gap. Wall  $y^+$  value is approximately 20. The working fluid used is air at ambient temperature and pressure as it is the same conditions in the cross flow experiment. Since the pressure drop through two fuel blocks is under 5000 Pa at maximum flow rate condition, the properties of fluid were kept constant for fast calculation. The Shear Stress Transport (SST) model of Menter (1994) [8] with an automatic wall treatment based on the Reynolds Averaged Navier-Stokes (RANS) equation was adopted for turbulence modeling. SST- $k-\omega$  shows good results for the flow with separation. In addition, the better results can be obtained by using the transitional Gamma-Theta

option [9]. The second order upwind scheme was implemented for the convective terms. Residual for convergence criteria of iteration was set under  $10^{-5}$ . The calculation conditions were set according to experimental conditions. The opening boundary condition was adopted to the upstream block and the cross gap between blocks, and the outlet of the downstream block is defined by the mass-flow-rate boundary condition. No slip wall and smooth wall were adopted as wall boundary conditions. Widths of the cross gaps were selected to be 0.5, 1, 2, 4, and 6 and outlet flow rates were determined to be 0.1 ~ 1.35 kg/s as in the experiment.

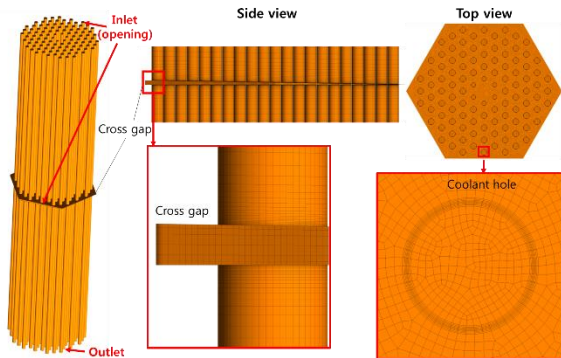


Fig. 3. Computational domain and mesh structure

#### 4. Results and Discussion

A series of experiments were performed in the test facility presented in section 2. The experimental cases were analyzed with the CFD model discussed in section 3 and the CFD results were compared with the experimental data for each case. This section describes the experimental results and the CFD calculation results.

##### 4.1 Comparison Results between CFD and Experiment

The experimental results and CFD calculation show good agreement as indicated in Fig. 4. The left graph of Fig. 4 shows the cross flow rate to the main flow rate in the case of gap width 6 mm. The cross flow rate increases with the main flow rate. Even though the cross flow rate seems to have linear relation, the ratio of the cross flow rate to the main flow rate decreases as the main flow rate increases as plotted in the right graph of Fig. 4. In the case of gap width 4 mm, the CFD prediction and experimental results are in good agreement as seen in Fig. 5. Even the CFD slightly underestimates the cross flow rate, the CFD calculation results are within uncertainty range. The trend of the results are consistent with that of the 6 mm gap width case.

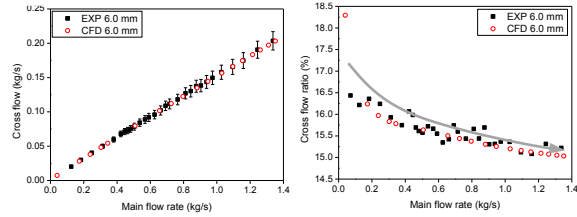


Fig. 4. Comparison results of gap width 6 mm case

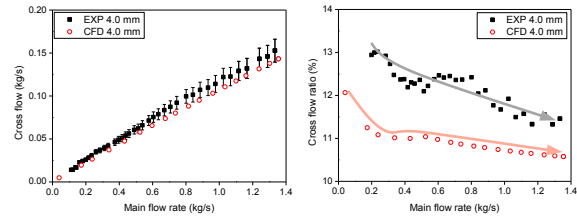


Fig. 5. Comparison results of gap width 4 mm case

In the case of gap width 2 mm, CFD slightly underestimates the cross flow rate as indicated in Fig. 6. The ratio of the cross flow rate shows different characteristics to the cases of gap width 6 mm and 4 mm. The ratio of the cross flow increases until main flow rate reaches 0.5 kg/s and decreases as the main flow rate increases. When the main flow rate reaches 0.5 kg/s, the Re number at the cross gap opening is approximately 2900. This results means that this region is laminar-turbulent transition region, which implies the tendency of the cross flow ratio is affected by flow regime. The discrepancy of the results between CFD calculation and experiment can be caused by laminar-turbulent transition. As described in Fig. 7, Fig. 8 and Fig 9, for velocity profile in the cross gap, the cross flow penetrates more deeply as the main flow rate increases. In the case of flow rate 0.224 kg/s, the cross flow is very weak and the flow converges to a center coolant hole. As the main flow rate increases, the cross flow penetrates deeper from opening. Therefore, it can be interpreted that the application of the turbulent model to the transitional flow regime, which is not valid for general turbulent models, can cause the calculation error. Nevertheless, the difference of the results is within 2%.

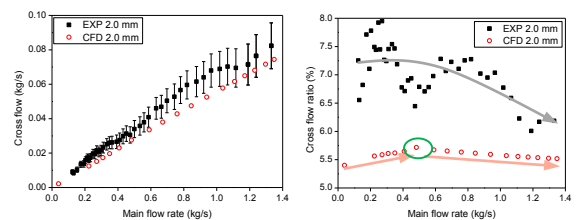


Fig. 6. Comparison results of gap width 2 mm case

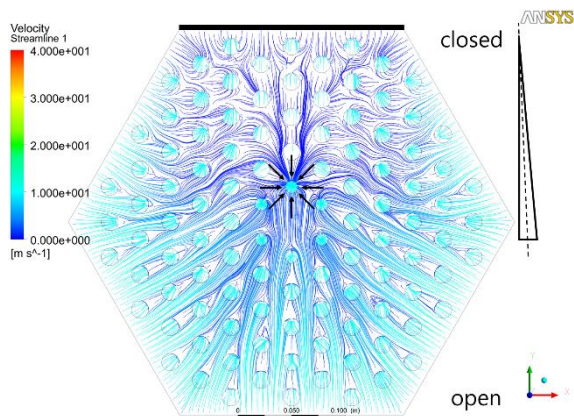


Fig. 7. Velocity streamline in the cross gap of 2 mm case, 0.224 kg/s main flow rate

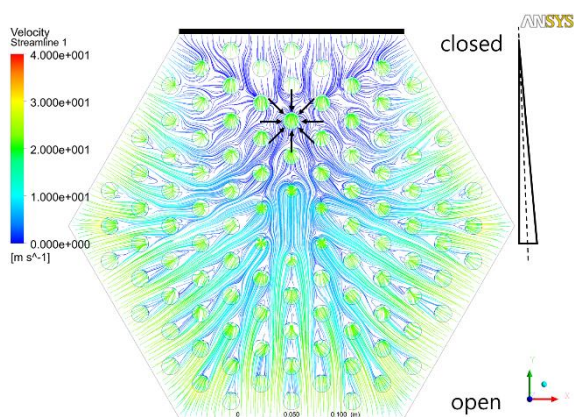


Fig. 8. Velocity streamline in the cross gap of 2 mm case, 0.5 kg/s main flow rate

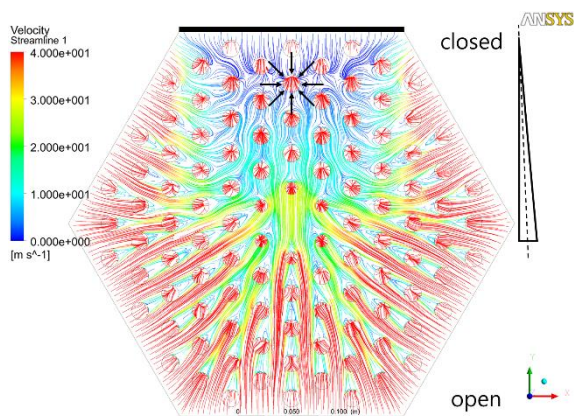


Fig. 9. Velocity streamline in the cross gap of 2 mm case, 1.35 kg/s main flow rate

In the case of gap width 1 mm, similar tendency is observed as seen in Fig. 10. The ratio of the cross flow increases until main flow rate reaches 0.9 kg/s and the Re number at the cross gap opening is approximately 2600. On the other hand, the ratio of the cross flow increases with the main flow rate in the case of gap width 0.5 mm as plotted in the right graph of Fig. 11. The Re number at the cross gap when the main flow rate is 1.35 is approximately 1700, which means the flow regime is dominantly laminar.

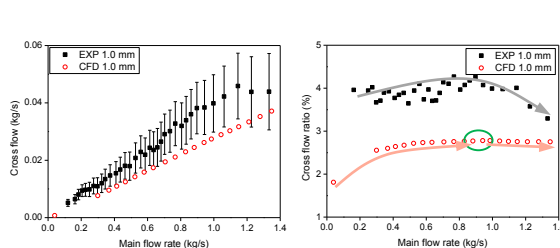


Fig. 10. Comparison results of gap width 1 mm case

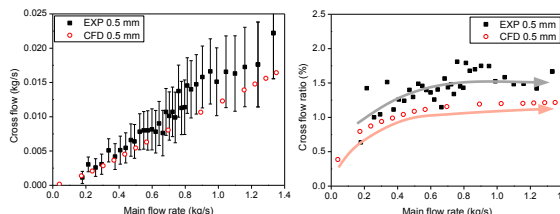


Fig. 11. Comparison results of gap width 0.5 mm case

The ratio of the cross flow for whole cases are plotted in Fig. 12. It is observed that the ratio of the cross flow is more significantly affected by the size of the cross gap than the main flow rate. Depending on the flow regime, the ratio of the cross flow shows different characteristics.

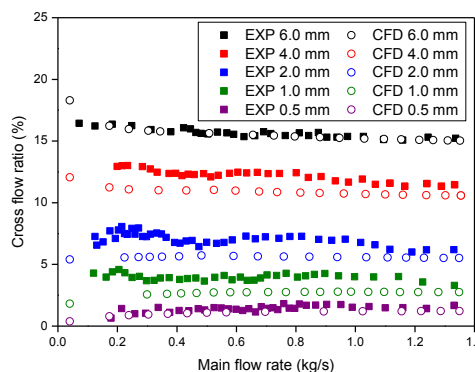


Fig. 12. The ratio of the cross flow in the cases of wedge-shaped gap

#### 4.2 Loss Coefficient

The loss coefficient of wedge-shaped gap is seen in Fig. 19. The loss coefficient is defined as

$$K = \frac{\Delta P}{\frac{1}{2} \rho v^2} \quad (1)$$

Where  $\Delta P$  is the pressure drop between the atmosphere and coolant channel at the cross gap and  $v$  is the velocity of the cross flow at the cross gap opening. In order to obtain the loss coefficient, the variables from CFD analysis results were used. When the main flow rate is high, the loss coefficient is nearly constant for different cross gap size. On the other hand, the loss coefficient varies with the cross gap size when the main flow rate is low. The same tendency is observed in the cases of parallel gap as shown in Fig. 20. It can be concluded that in high Re region, the loss coefficient is almost constant whereas it varies with the gap size in low Re region.

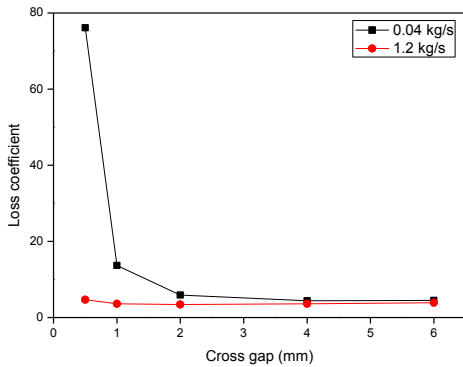


Fig. 19: Loss coefficient of wedge-shaped gap

## 5. Conclusion

In the present paper, in order to understand the cross flow phenomena in the core of PMR200, the cross flow experimental facility was constructed. Wedge-shaped gap were used for the experiments and the cross flow rates were measured varying gap size and flow rate. In addition, CFD analysis was performed to validate the capacity of CFD prediction and to observe local phenomena. Conclusions can be summarized as follows:

- Results of the CFD analysis and experimental data are in good agreement even though CFD slightly underestimates in laminar-turbulent transitional region.
- The ratio of cross flow is more affected by the cross gap size than by the main flow rate.
- The loss coefficient is nearly constant in high Re region whereas it varies with the gap size in low Re region.

In this study, the pressure loss coefficient for the cross gap between the fuel blocks of PMR200 was derived. Further study will be followed to develop the correlation of the cross flow loss coefficient, and then the correlation will be used to other thermal-hydraulic analysis codes for prismatic VHTR that incorporate lumped parameter model.

## Acknowledgement

This work was supported by a Basic Atomic Energy Research Institute (BAERI) grant funded by the Korean government Ministry of Education and Science Technology (MEST) (grant 20100018759)

## REFERENCES

- [1] J. C. Gauthier, G. Brinkmann, B. Copsey, M. Lecomte, ANTARES: The HTR/VHTR project at Framatome ANP, Nuclear Engineering and Design, Vol.236, pp.526-533, 2006.
- [2] C. K. Jo, H. S. Lim, J. M. Noh, Preconceptual Designs of the 200 MWth Prism and Pebble-bed Type VHTR Cores, Proceedings of International Conference on the Physics of Reactors 2008, 14-19 Sep. 2008, Interlaken, Switzerland.

- [3] A. Baxter, C. Rodriguez, M. Richards, J. Kuzminski, Helium-Cooled Reactor Technologies for Accelerator Transmutation of Nuclear Waste, Proceedings of 6<sup>th</sup> Information Exchange Meeting on Actinide and Fission Product Partitioning and Transmutation 2000, Dec. 11-13, 2000, Madrid, Spain.

- [4] Idaho National Engineering and Environmental Laboratory, NGNP Preliminary Point Design – Results of the Initial Neutronics and Thermal-Hydraulic Assessment, INEEL/EXT-03-00870, USA, 2003.

- [5] H. G. Groehn, Estimate of Cross Flow in High Temperature Gas-cooled Reactor Fuel Blocks, Heat Transfer and Fluid Flow, Nuclear Technology, Vol.5, pp.392-400, 1982.

- [6] H. Kaburaki, T. Takizuka, Crossflow Characteristics of HTGR Fuel Blocks, Nuclear Engineering and Design, Vol.120, pp.425-434, 1990.

- [7] J. H. Lee, S. J. Yoon, E. S. Kim, G. C. Park, CFD Analysis and Assessment for Cross-flow Phenomena in VHTR Prismatic Core, Heat Transfer Engineering, Vol.35, pp.1151-1160, 2014.

- [8] F. R. Menter, Two-equation Eddy-viscosity Turbulence Models for Engineering Applications, AIAA Journal, Vol.32, pp.1598-1605, 1994.

- [9] R. B. Langtry, F. R. Menter, Transition Modeling for General CFD Applications in Aeronautics, AIAA Journal, Proceedings of 43<sup>rd</sup> AIAA Aerospace Sciences Meeting, 10-13 Jan. 2005, Reno, NV, USA.